AMERICAN SOCIETY FOR MICROBIOLOGY | Applied and Environmental Microbiology®

ENVIRONMENTAL MICROBIOLOGY

Hydrogen Does Not Appear To Be a Major Electron Donor for Symbiosis with the Deep-Sea Hydrothermal Vent Tubeworm *Riftia pachyptila*

Jessica H. Mitchell,[a] Juliana M. Leonard,[b] Jennifer Delaney,[a] Peter R. Girguis,[a] Kathleen M. Scott[b]

[a]Department of Organismic and Evolutionary Biology, Harvard University, Cambridge, Massachusetts, USA
[b]Department of Integrative Biology, University of South Florida, Tampa, Florida, USA

Jessica H. Mitchell and Juliana M. Leonard contributed equally to this article.

ABSTRACT Use of hydrogen gas (H_2) as an electron donor is common among free-living chemolithotrophic microorganisms. Given the presence of this dissolved gas at deep-sea hydrothermal vents, it has been suggested that it may also be a major electron donor for the free-living and symbiotic chemolithoautotrophic bacteria that are the primary producers at these sites. Giant *Riftia pachyptila* siboglinid tubeworms and their symbiotic bacteria ("*Candidatus* Endoriftia persephone") dominate many vents in the Eastern Pacific, and their use of sulfide as a major electron donor has been documented. Genes encoding hydrogenase are present in the "*Ca*. Endoriftia persephone" genome, and proteome data suggest that these genes are expressed. In this study, high-pressure respirometry of intact *R. pachyptila* and incubations of trophosome homogenate were used to determine whether this symbiotic association could also use H_2 as a major electron donor. Measured rates of H_2 uptake by intact *R. pachyptila* in high-pressure respirometers were similar to rates measured in the absence of tubeworms. Oxygen uptake rates in the presence of H_2 were always markedly lower than those measured in the presence of sulfide, as was the incorporation of ^{13}C-labeled dissolved inorganic carbon. Carbon fixation by trophosome homogenate was not stimulated by H_2, nor was hydrogenase activity detectable in these samples. Though genes encoding [NiFe] group 1e and [NiFe] group 3b hydrogenases are present in the genome and transcribed, it does not appear that H_2 is a major electron donor for this system, and it may instead play a role in intracellular redox homeostasis.

IMPORTANCE Despite the presence of hydrogenase genes, transcripts, and proteins in the "*Ca*. Endoriftia persephone" genome, transcriptome, and proteome, it does not appear that *R. pachyptila* can use H_2 as a major electron donor. For many uncultivable microorganisms, omic analyses are the basis for inferences about their activities *in situ*. However, as is apparent from the study reported here, there are dangers in extrapolating from omics data to function, and it is essential, whenever possible, to verify functions predicted from omics data with physiological and biochemical measurements.

KEYWORDS hydrogenase, deep-sea hydrothermal vent, siboglinid, *Riftia pachyptila*, invertebrate-microbe interactions

Hydrogen gas (H_2) is an electron-donating substrate for microbial energy generation in a variety of chemosynthetic habitats, such as mangroves, shallow sediments, hydrothermal vents, hydrocarbon seeps, and whale falls (1–3). At vents, H_2 can reach micromolar concentrations up to tens to hundreds, depending on the site (4–6). In

Citation Mitchell JH, Leonard JM, Delaney J, Girguis PR, Scott KM. 2020. Hydrogen does not appear to be a major electron donor for symbiosis with the deep-sea hydrothermal vent tubeworm *Riftia pachyptila*. Appl Environ Microbiol 86:e01522-19. https://doi.org/10.1128/AEM.01522-19.

Editor Harold L. Drake, University of Bayreuth

Address correspondence to Kathleen M. Scott, kmscott@usf.edu.

Received 4 July 2019
Accepted 9 October 2019
Accepted manuscript posted online 18 October 2019
Published 13 December 2019

these environments, H_2 is used by methanogens, acetogens, and a diversity of other microbes for energy generation (7–9).

Hydrogenases mediate the reaction $H_2 \rightleftharpoons 2\,H^+ + 2e^-$ and are found across all three domains of life (10). Hydrogenases are classified according to their catalytic metal centers: the [FeFe] hydrogenases, the [NiFe] hydrogenases, and the [Fe] hydrogenases, the last being found only in some methanogenic archaea. The three classes differ with respect to gene organization, location within the cell, and function. Many of these enzymes are known to be bidirectional, but in general the [FeFe] hydrogenases are involved in H_2 evolution, whereas the [NiFe] hydrogenases are involved in H_2 consumption (10, 11). Studies in the last few years have shown that some hydrogenases are capable of electron bifurcation and are even involved in extracellular electron transfer (12–14). However, the physiological function of hydrogenases in many organisms remains putative due to their limited representation among cultivated microbes, the modular nature of how hydrogenases are assembled, and the fact that the direction of electron flow through these enzymes is dependent on the electrochemical potential near their catalytic sites (10, 15–17).

Symbioses between chemoautotrophic bacteria and eukaryotic hosts are ubiquitous in many of the ecosystems in which H_2 is found (18). Among most of these symbioses, inorganic electron donors and acceptors are used to regenerate ATP and reducing equivalents for microbial growth and biosynthesis. Moreover, the symbionts assimilate inorganic carbon and "fix" it into metabolic precursors (e.g., simple organic acids) that are typically translocated to the host (19–22). The animals, in turn, use this carbon for their own bioenergetic and biosynthetic needs. The efficacy of these associations is apparent in the abundance of symbioses in many chemosynthetic habitats; indeed, carbon fixation by these associations contributes substantially to net primary productivity at vents (23).

To date, many studies have focused on the use of hydrogen sulfide (here referred to as ΣH_2S) by the symbionts of these associations (24), but more recently the palette of electron donors has grown to include H_2 (1, 25). Symbionts of the mussel *Bathymodiolus puteoserpentis* have been shown via genomic analyses, environmental geochemical measurements, and H_2-dependent carbon fixation to definitively use hydrogenases for harnessing energy from H_2 oxidation (1). Transcriptomic and proteomic studies have even found that the symbionts of the giant hydrothermal vent tubeworm *Riftia pachyptila* express putative hydrogenase genes and proteins, respectively (2, 26–28). *R. pachyptila* flourishes at deep-sea hydrothermal vents in the Eastern and Southeastern Pacific and is a foundational species that supports high productivity rates and provides habitat for many other vent fauna. *R. pachyptila* is a siboglinid worm that forms an obligate symbiosis with "*Candidatus* Endoriftia persephone" (27, 29–31), a member of *Gammaproteobacteria*. *R. pachyptila* lacks a mouth, gut, and anus and derives most, if not all, of its nutrition from its symbionts. Early studies of *R. pachyptila* tested the utilization of multiple potential electron donors, including H_2, but it was observed that only ΣH_2S stimulated carbon fixation under their test conditions. That said, earlier studies were limited to measuring substrate uptake and carbon fixation in excised symbiont-containing tissues incubated at 1 atm (32). The importance of ΣH_2S to *R. pachyptila*'s symbionts was further underscored by the abundance of sulfide-binding proteins in the worm's blood (33, 34), as well as the presence of elemental sulfur among the symbionts (35, 36). These observations, along with the measured stimulation of carbon fixation in the presence of ΣH_2S, emphasized the role of ΣH_2S as the symbiont's primary electron donor (23, 37, 38).

Nevertheless, the more recent transcriptomic and proteomic studies call into question the relevance of H_2 to symbiont function. H_2 is present in the hydrothermal fluid bathing *R. pachyptila in situ*, at concentrations ranging up to $\sim$25 μM (4, 39). In basalt hosted vent sites where *R. pachyptila* is found, the majority of the available catabolic energy comes from ΣH_2S; nevertheless, H_2 oxidation does occur and represents $\sim$5 to 20% of total available energy in the fluid surrounding *R. pachyptila* (4). Supplementation of sulfide-driven primary productivity with H_2 use by *R. pachyptila* could be an

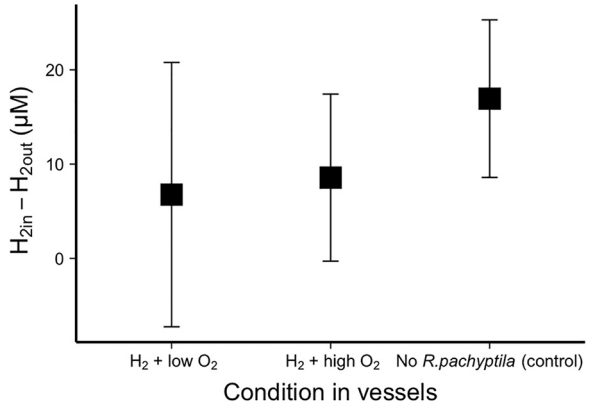

FIG 1 H_2 uptake by *R. pachyptila* compared to vessels without *R. pachyptila* (control), calculated using the least square (LS) means of the difference in H_2 concentrations in the seawater entering and leaving the pressure vessels. For the control, vessels without *R. pachyptila* were supplied with H_2 gas (~100 μM) with either low (~30 μM) or high (~250 μM) O_2 concentrations. Data from these control vessels were aggregated, as no significant difference of uptake was found between them. Furthermore, no significant difference was found in H_2 uptake when comparing control vessels to those containing *R. pachyptila* ($\alpha = 0.05$).

important aspect of this symbiosis and could plausibly contribute to *R. pachyptila*'s remarkable growth rates, which, in turn, lead to its flourishing at high densities around vents and playing a key role in structuring the vent ecosystem. The aforementioned presence of putative hydrogenases and the recognition that earlier studies lacked the ability to replicate *in situ* conditions led us to reevaluate the possible relevance of H_2 oxidation to the energy metabolism of the *R. pachyptila* symbiont.

Therefore, the purpose of this study was to determine if the *R. pachyptila* symbionts could use H_2 as an electron donor for chemolithoautotrophy. With that in mind, we conducted live-animal and symbiont-containing tissue incubations with or without H_2, comparing rates of O_2, ΣH_2S, and H_2 consumption, as well as carbon fixation. In addition, hydrogenase assays were performed to measure enzyme activities in symbiont-containing tissues, and the presence and transcription of hydrogenase genes from the symbiont genomes were noted.

RESULTS

Respirometry. H_2 consumption in aquaria with *R. pachyptila* was not significantly different from that in control aquaria without *R. pachyptila* (Fig. 1). The two control aquaria (H_2 with low and high O_2 concentrations) were aggregated for this comparison, as no significant difference was found between them using a Welch two-sample test ($\alpha = 0.05$). The least square (LS) means of H_2 uptake between aquaria with *R. pachyptila* and the aggregated aquaria without tubeworms (control aquaria) were calculated using a generalized least square model in R, and these least square means were compared using a pairwise-adjusted Holmes test, with an α value of 0.05 (40). O_2 uptake rates in aquaria supplied with H_2 were lower than in the case of treatments with ΣH_2S. This was true for both high and low O_2 concentrations (Fig. 2).

Carbon fixation by *R. pachyptila* symbioses maintained in high-pressure aquaria with either H_2 or ΣH_2S as an electron donor. Dissolved inorganic carbon (DIC) incorporation into biomass (i.e., carbon fixation) by *R. pachyptila* incubated in the presence of H_2 gas was 5- to 23-fold lower than in treatments in which *R. pachyptila* was given adequate ΣH_2S and O_2 (Fig. 3 and 4). The rates of carbon fixation for both H_2 treatments were indistinguishable from those measured when *R. pachyptila* was maintained under low-O_2 conditions (Fig. 4).

Dissolved inorganic carbon incorporation by trophosome samples. Trophosome samples from an *R. pachyptila* individual maintained in the presence of H_2 did not have elevated carbon fixation rates relative to that of the control (Fig. 5). Homogenized trophosome samples from this individual had similar rates of carbon fixation when

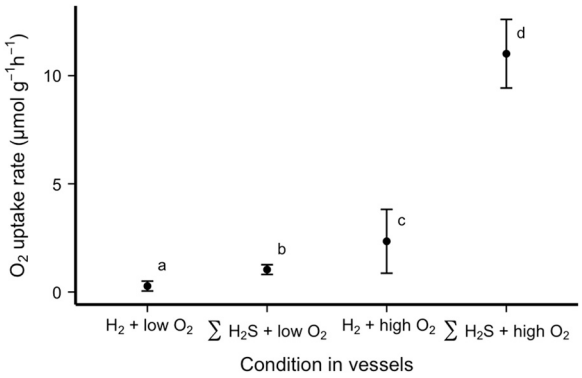

FIG 2 Least squares means of O_2 uptake rates by *R. pachyptila* incubated in vessels in the presence of H_2 or ΣH_2S. Letters indicate data that differed statistically significantly ($\alpha = 0.05$).

incubated in the presence (0.034 ± 0.004 nmol of CO_2 min^{-1} mg of protein) or absence (0.037 ± 0.002 nmol of CO_2 min^{-1} mg of protein) of H_2. Carbon fixation was stimulated solely when ΣH_2S was added (0.067 ± nmol min^{-1} mg of protein [Fig. 5]).

When regressing carbon fixed against incubation time, inclusion of indicator variables for electron donors significantly reduced the residual sum of squares ($F = 87$; $P < 0.001$). Values of β_3 and β_5 from the full model (see Materials and Methods) were statistically distinguishable from zero ($P = 0.003$ and 0.04, respectively), indicating that ΣH_2S significantly stimulated carbon fixation, while values of β_3 and β_5 were not, indicating that the amount of carbon fixed when H_2 was added could not be distinguished from the amount fixed in its absence.

Hydrogenase activity. Neither freshly collected *R. pachyptila* worms nor those that had been maintained in high-pressure aquaria with H_2 had measurable hydrogenase activity in trophosome samples (Table 1). Assay mixtures of some of the *R. pachyptila* samples grew slightly more turbid over the 5-min assay time course, which is reflected in the small negative values for these samples. Hydrogenase activity was apparent in *Hydrogenovibrio thermophilus* MA2-6; the presence of H_2 significantly increased the rate of methylene blue reduction ($P < 0.001$).

Hydrogenase genes in the "*Ca*. Endoriftia persephone" genome. The "*Ca*. Endoriftia persephone" genomes from *R. pachyptila*, *Tevnia jerichonana*, and *Ridgeia piscesae* include genes homologous to those for four types of hydrogenase (IMG gene object identifier numbers 2600441592, 2600441595, 2600436887, and 2601634699). Using the classification and E values calculated by comparing these sequences to those in HydDB, these include [FeFe] group C1 (E value $< 4e^{-5}$), [FeFe] group C3 (E value $< 7e^{-5}$), [NiFe] group 1e Isp type (as previously described in reference 41; E value = 0), and [NiFe] group 3b (E value = 0) (Fig. 6).

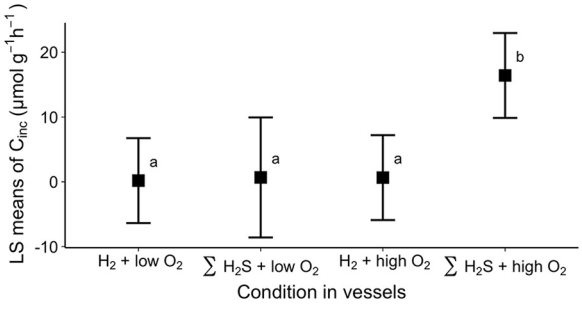

FIG 3 LS means of inorganic carbon incorporation rates (C_{inc}) by *R. pachyptila* incubated in vessels in the presence of H_2 or ΣH_2S. Means were computed from data from individuals in Fig. 4. Letters indicate data that differed statistically significantly ($\alpha = 0.05$).

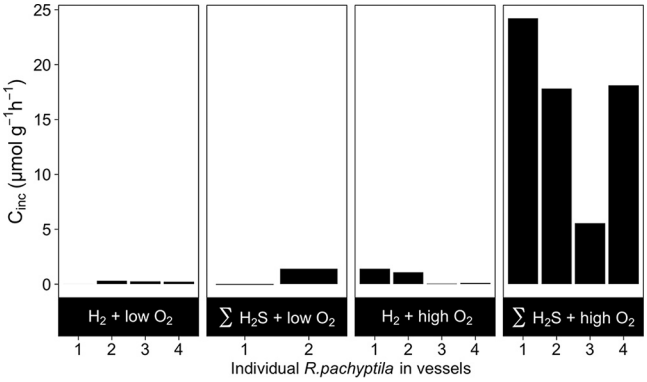

FIG 4 Inorganic carbon incorporation rate (C_{inc}) for individual *R. pachyptila* tubeworms incubated in the presence of H_2 or ΣH_2S with low or high O_2 concentrations.

Abundances of hydrogenase transcripts. Transcriptome sequencing with Novaseq resulted in an average of ~62 million reads per sample, with ~36 million left after trimming. Between 3 and 27% (average 15%) of these reads pseudoaligned to "*Ca*. Endoriftia persephone" coding DNA sequence (CDS) regions. Hydrogenase genes from type 1e and 3b were transcribed in all samples (Fig. 7; see also Table S1 in the supplemental material).

Differences in the relative abundances of transcripts encoding type 1e hydrogenase were apparent in two of the treatment comparisons: (i) when O_2 was high, these transcripts were more abundant in the presence of H_2 than in the presence of ΣH_2S, and (ii) when ΣH_2S was present and H_2 was absent, these transcripts were more abundant under low-O_2 conditions than under high-O_2 conditions. Transcript abundances for the type 3b hydrogenase were also elevated under the second set of conditions (Table 2).

DISCUSSION

H_2 does not appear to be a major electron donor for the *R. pachyptila* symbiosis. Intact *R. pachyptila* maintained at quasi-*in situ* conditions does not use significant quantities of H_2. Moreover, the presence of H_2 does not stimulate O_2 consumption or carbon fixation by intact *R. pachyptila* or in excised and incubated trophosome samples. Furthermore, hydrogenase activities, specifically H_2-dependent methylene blue reduction, were not measurable in trophosome samples.

Hydrogenase genes are likely to encode active hydrogenase enzymes and are transcribed and expressed. The absence of evidence for H_2 utilization by this symbiosis is puzzling given the presence of genes encoding multiple hydrogenase enzymes in the "*Ca*. Endoriftia persephone" genome. The two [NiFe] hydrogenase large subunit

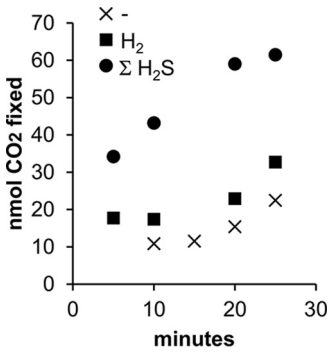

FIG 5 CO_2 fixation by homogenized trophosome samples in the absence (-) and presence of 0.16 mM H_2 or 0.11 mM H_2S.

TABLE 1 Hydrogenase activities of trophosome samples and cultivated bacteria

Species	Specimen conditions before harvest	Assay headspace gas	Activity (mmol of H_2 min^{-1} mg of $protein^{-1}$)[a]	n[b]
H. thermophilus MA2-6	Batch culture with H_2	H_2	0.39	1[c]
	Batch culture with H_2	Ar	0.12	1
	Batch culture with H_2	H_2	1.48	1
	Batch culture with H_2	Ar	0.00	1
R. pachyptila 1[d]	Freshly collected	H_2	−0.001 ± 0.002	3
R. pachyptila 2	Freshly collected	H_2	−0.006 ± 0.007	2
R. pachyptila 3	Freshly collected	H_2	0.000 ± 0.003	2
R. pachyptila 4	Aquaria with H_2	H_2	−0.006 ± 0.005	2
R. pachyptila 5	Aquaria with H_2	H_2	−0.004 ± 0.003	2
R. pachyptila 6	Aquaria with H_2	H_2	−0.001 ± 0.004	2

[a]Values are means ± standard deviations.
[b]*n*, number of times activity was measured for a particular culture or individual.
[c]For the *H. thermophilus* MA2-6 samples, values measured in the presence of H_2 gas were statistically different ($P < 0.001$) from those measured in the presence of Ar.
[d]*R. pachyptila* 1 to 6 are six different individuals.

genes include signature sequences suggesting catalytic activity of their protein products as hydrogenase. The amino acid sequence predicted from the gene encoding the [NiFe] group 1e hydrogenase large subunit has matches to the L1 and L2 signature sequences present in other group 1e members (11). The sequence predicted from the gene encoding the [NiFe] group 3b hydrogenase also has matches to L1 and L2 signature sequences from group 3b, but these matches are not exact. However, they do include the two CXXC motifs of the active site of this enzyme (11). The gene neighborhoods of these [NiFe] hydrogenase large-subunit genes provide further evidence for hydrogenase activity. Both large-subunit genes are colocated with genes encoding hydrogenase small subunits (41) (Fig. 6). For the group 1e hydrogenase genes, genes

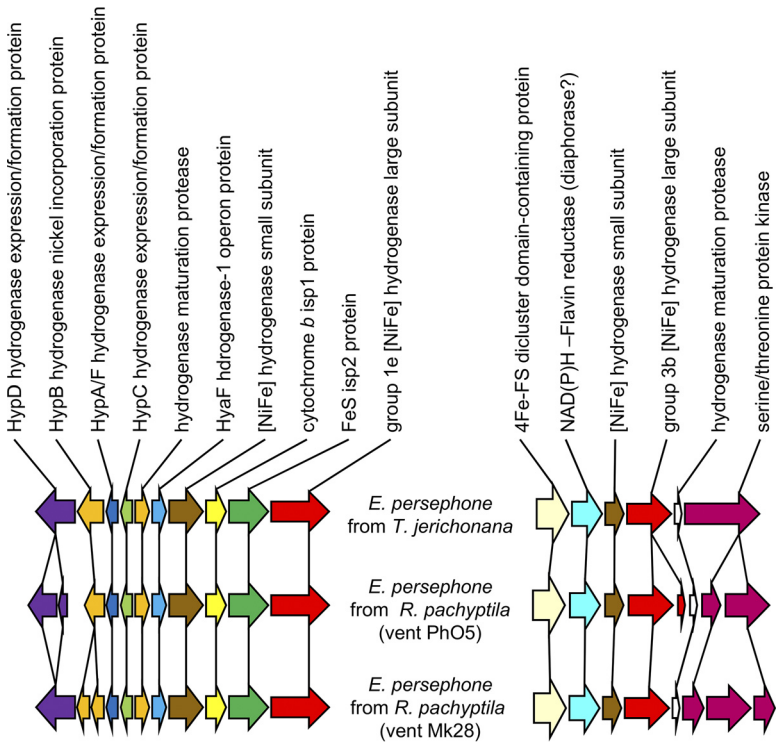

FIG 6 Gene synteny near putative group 1e and 3b [Ni Fe] hydrogenase genes among "*Ca*. Endoriftia persephone." The genes depicted include IMG gene object identifier (ID) numbers 2600441718 to 2600441727 and 2600441763 to 2600441768 (*T. jerichonana*), 2600436877 to 2600436887 and 2600438609 to 2600438602 (*R. pachyptila* vent Ph05), and 2601634007 to 2601633997 and 2601634696 to 2601634703 (*R. pachyptila* vent Mk28).

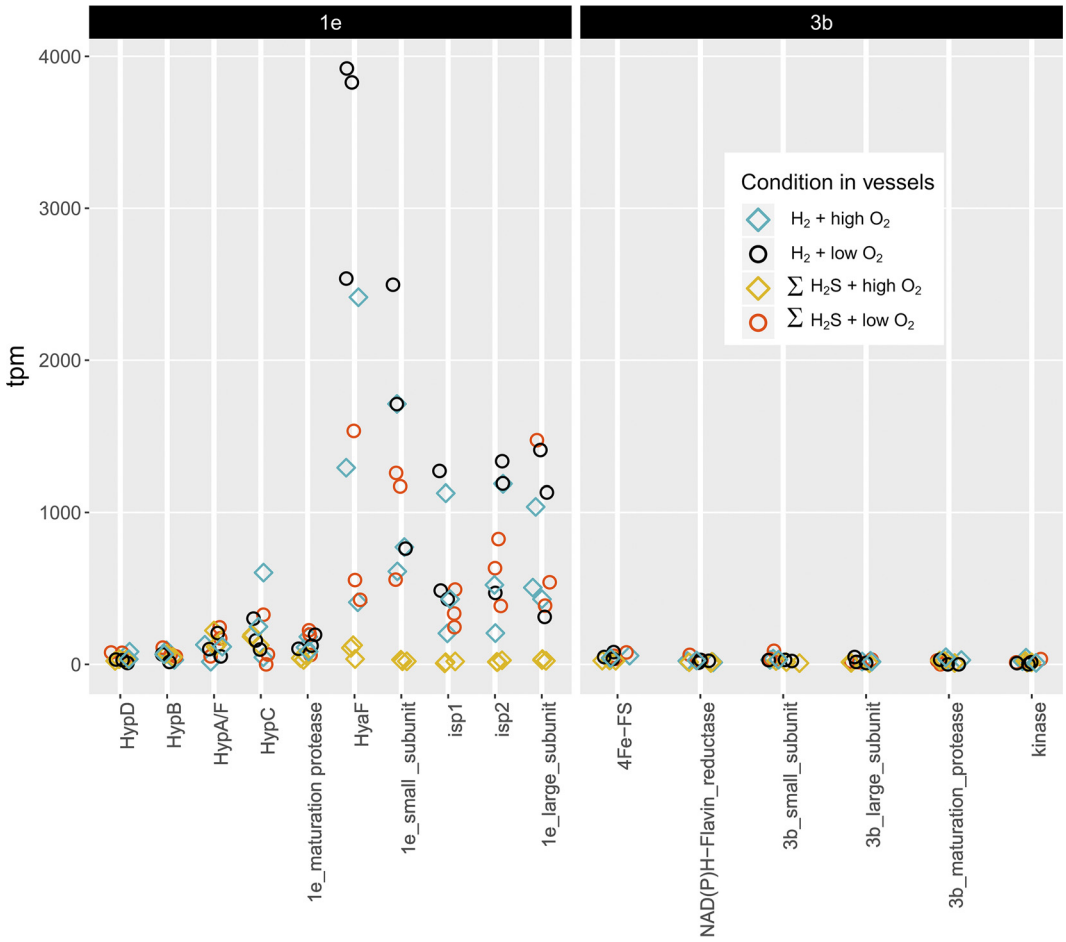

FIG 7 Transcripts per million (tpm) encoding type 1e (left) and 3b (right) hydrogenase subunits and associated proteins for RNA extracted from trophosome samples from *R. pachyptila* incubated in the presence of H_2 and ΣH_2S under low- and high-O_2 conditions.

encoding accessory proteins necessary for their assembly are also nearby (41). Genes encoding the two [NiFe] hydrogenases are indeed expressed in "*Ca*. Endoriftia persephone" while present *in hospite* (2, 26–28), and the presence of transcripts of genes encoding both 1e and 3b hydrogenases is consistent with expression *in hospite* (Table 2

TABLE 2 Differential abundance of transcripts encoding hydrogenase subunits and regulatory proteins in "*Ca*. Endoriftia persephone"

Hydrogenase type	Predicted protein[a]	β (qval)[d]			
		$H_2/\Sigma H_2S$[b]		Low O_2/high O_2[c]	
		High O_2	Low O_2	H_2	ΣH_2S
Type 1e	HypD	1.12 (4.0×10^{-3})			0.80 (2.1×10^{-2})
	1e maturation protein				1.28 (3.0×10^{-2})
	HyaF	2.73 (4.8×10^{-4})	1.53 (4.60×10^{-2})		2.30 (6.5×10^{-4})
	1e small subunit	3.74 (4.8×10^{-23})			3.73 (8.7×10^{-35})
	Isp1	3.66 (5.9×10^{-8})			3.34 (7.7×10^{-17})
	Isp2	3.37 (4.7×10^{-8})			3.50 (1.3×10^{-29})
	1e large subunit	3.10 (5.3×10^{-20})			3.17 (4.3×10^{-12})
Type 3b	4Fe-S				0.82 (2.0×10^{-2})
	NAD(P)H-flavin reductase				1.11 (4.5×10^{-2})
	3b small subunit				1.26 (2.4×10^{-2})

[a]Proteins on the 1e and 3b contig that did not show any significant differential transcript abundance are not included.
[b]Comparison of transcript levels in the presence of H_2 (numerator) or ΣH_2S (denominator), under either low or high O_2 concentrations.
[c]Comparison of transcript levels in the presence of low (numerator) or high (denominator) concentrations of O_2, when either H_2 or ΣH_2S was provided.
[d]β is the $\log_2$ fold change relative to the treatment indicated in the denominator of the compared treatments (a/b). qval is the *P* adjusted value with a cutoff of 0.05.

and Fig. 7). Furthermore, when differences in transcript abundance are apparent, transcripts encoding all four subunits of the type 1e hydrogenase are upregulated by similar amounts, suggesting that this enzyme is assembled as predicted, though protein abundances were not measured via proteomic or Western blot analyses.

While two potential [FeFe] hydrogenase genes from "*Ca*. Endoriftia persephone" are likely to share evolutionary history with group C1 and C3 [FeFe] hydrogenases, these two genes lack sequence signatures L1Fe, L2Fe, and L3Fe conserved among other [Fe Fe] hydrogenases and implicated in active-site architecture (11), raising doubt that the proteins encoded by these genes are catalytically active as hydrogenases.

Potential reasons for lack of evidence for H_2 use as a major electron donor by the *R. pachyptila* symbiosis. It is possible that hydrogenase activity was present but not measureable in our assay, in which methylene blue was used as an electron acceptor. Many (42) but not all (43) hydrogenases are capable of reducing methylene blue. It is also possible that reduced methylene blue was not stable in crude cell extract prepared from trophosome samples. However, the possibility that substantial uptake hydrogenase activity was present in these samples seems unlikely, given that the presence of H_2 does not stimulate metabolic activities of intact *R. pachyptila* (Fig. 1 and 4) or "*Ca*. Endoriftia persephone" (Fig. 5).

Another reason for an absence of apparent use of H_2 as a major electron donor, despite the presence of hydrogenase-encoding genes, in "*Ca*. Endoriftia persephone" may be that this microorganism differentially expresses them based on its lifestyle. "*Ca*. Endoriftia persephone" is environmentally transmitted between generations of *R. pachyptila* (44, 45) and therefore spends some time as a free-living microorganism. It may be possible that this microorganism can use H_2 as a major electron donor when it is free-living but not when it is symbiotic with *R. pachyptila*.

It is also possible that these [NiFe] hydrogenases function primarily to maintain intracellular redox homeostasis *in hospite*. Both [NiFe] group 1e and 3b enzymes are reversible, capable of H_2 production (11, 46). Some group 3b hydrogenases couple the oxidation of NADPH to evolution of H_2 (11, 47) and are upregulated under hypoxia to maintain an optimal balance of reduced and oxidized cofactors, such as NAD^+/NADH (48). Transcript levels are consistent with hydrogenase playing a role in redox homeostasis in "*Ca*. Endoriftia persephone." Under high-O_2 conditions, transcript abundances were higher when H_2 was present, but transcript abundances were also elevated when ΣH_2S was the sole electron donor provided and O_2 concentrations were low (Fig. 7 and Table 2). In both cases, the symbionts may have been responding to a lack of (i) reductant or (ii) oxidant, which supports the hypothesis that these hydrogenases may play a role in redox homeostasis.

Conclusions and perspectives. Altogether, the lack of physiological response of "*Ca*. Endoriftia persephone" to the provision of H_2—both *in hospite* and *in vitro*—is not consistent with the hypothesis that H_2 is an electron donor for energy metabolism. More specifically, the provision of H_2 does not lead to increased oxygen demand, nor does it stimulate carbon fixation. In contrast, previous studies have consistently shown that the provision of sulfide, for example, both increases oxygen utilization and stimulates carbon fixation. The genomic and transcriptome analyses are consistent with the presence of biochemically active hydrogenases, which may play a role in intracellular redox homeostasis. Therefore, hydrogenase activity would not likely stimulate carbon fixation, nor would it need to be present at high activity levels necessary if H_2 was a major source of electrons for autotrophy; this could explain why the presence of this gas did not measurably stimulate symbiont CO_2 fixation.

Previous omics work had strongly suggested that the ecosystem-structuring *R. pachyptila* symbiosis could use H_2 as an energy source/electron donor. This study casts doubt on this possibility, and also provides a cautionary tale about extrapolating from omics data to system function/physiology. This is quite timely given the growing importance of omics data, particularly for the as-of-yet-uncultivable majority of ecologically and environmentally relevant microorganisms.

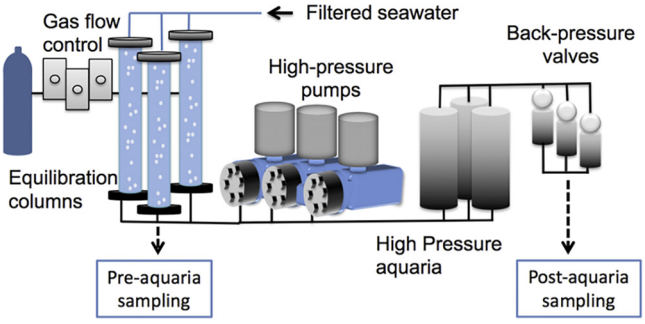

FIG 8 Schematic of the high-pressure respirometry system. Selected gases (e.g., H_2, H_2S, CO_2, O_2, and N_2) are bubbled into equilibration columns that feed high-pressure pumps, which, in turn, pump fluid into aquaria. Pressure is controlled via back-pressure/relief valves which allow for a flowthrough system.

MATERIALS AND METHODS

***R. pachyptila* collection.** *R. pachyptila* worms were collected during an expedition in October of 2016 on board the *RV Atlantis* to the hydrothermal vents at the 9°N Integrated Study Site in the East Pacific (9°50′N, 104°18′W, 2,500 m). *R. pachyptila* worms were collected via the human-occupied vehicle (HOV) *Alvin* during dives to the sites Tica and Bio 9. Live worms were stored in a thermally insulated container during submersible transit to the surface and were sorted in ice-cold seawater or dissected immediately upon recovery.

High-pressure respirometry system. The high-pressure respirometry system (HPRS) resides in a 20-foot refrigerated intermodal shipping container. This system allows for the incubation of hydrothermal vent animals at temperatures, pressures, and water chemistries that reflect *in situ* conditions. This was accomplished by using Aalborg mass flow controllers to bubble gases (H_2, H_2S, CO_2, and O_2, with N_2 as a carrier gas) through 0.2-μm-filter-sterilized seawater contained within 1-m-tall gas equilibration columns to recreate the chemical conditions *in situ*. This gas-amended seawater was then fed to high-pressure pumps (Lewa America, Inc.) which delivered this fluid into custom-built 3-liter titanium high-pressure aquaria in which the tubeworms were kept. Pressure was maintained in the aquaria with stainless steel back-pressure/relief valves (Straval, Inc.) that allow for a flowthrough rate of ~50 ml·min^{-1} at a constant pressure of ~27.5 MPa (Fig. 8).

Incubation conditions and respirometry. *R. pachyptila* worms that were quick to withdraw into their tubes when lightly touched were selected for shipboard incubations in the HPRS. Four to six tubeworms were placed into each high-pressure aquarium and were provided with either H_2 or ΣH_2S as an electron donor, at high and low O_2 concentrations (Table 3). To measure consumption of dissolved gases, water samples were collected from the equilibration columns that supplied the aquaria (intake, or pre-aquarium sampling) and from the back-pressure valve located downstream of the aquaria (outake, or post-aquarium sampling). Dissolved H_2 was measured with a Unisense H_2 minisensor 500 (range = 0 to 800 μM; detection limit = 0.3 μM) encased in a glass flowthrough cell that was placed in-line with the intake or outtake of the aquaria. O_2 was measured using a PreSens oxygen FTC-SU-PSt3-S flowthrough cell (range = 0 to 1,400 μM). ΣH_2S (the sum of the sulfide species $H_2S + HS^- + S^{2-}$) was qualitatively measured aboard ship by colorimetric analysis (49; LaMotte sulfide test kit). Subsamples were also preserved in a 2 mM zinc acetate solution and shipped to the lab, where they were stored at −80°C until analysis. For lab-based ΣH_2S quantification, the frozen samples were thawed and vortexed, and 100 μl was pipetted into a 96-well clear-bottom plate. Eight microliters of reagent A (LaMotte sulfide test kit) and 2.5 μl of reagent B were added per sample, mixed, and aliquoted into a 96-well plate ~1 min before the absorbance was read at 670 nm with a Spectramax i3 plate reader.

Upon cessation of experiments, aquaria were slowly depressurized and tubeworms were removed, weighed on a motion-compensated shipboard balance (50), and dissected in a cold room (~4°C). Tissue samples were taken from the trophosome (symbiont containing) and the plume, vestimentum, and skin (nonsymbiont containing) for isotope incorporation analysis, RNA preservation, and enzyme assays. Samples used for trophosome incubations were processed immediately onboard the ship, as were those

TABLE 3 Incubation conditions for *R. pachyptila* maintained in the high-pressure respirometry system

Treatment[a]	H_2 (μM)	ΣH_2S[b] (μM)	O_2 (μM)	n[c]	Total biomass (g)	Biomass range (g)	Duration (h)
H_2 + high O_2	114 ± 5	0	272 ± 42	5 (0)	177	31–65	64
H_2 + low O_2	113 ± 12	0	31 ± 5	5 (1)	222	29–40	64
ΣH_2S + high O_2	0	148 ± 33	291 ± 11	6 (0)	48.14	2.4–16	52
ΣH_2S + low O_2	0	159 ± 34	32 ± 8	4 (1)	66.7	6.0–33.7	52

[a]Dissolved gas concentrations are the averages of measurements taken from the equilibration columns every 4 h ± standard deviations.
[b]$\Sigma H_2S = [H_2S] + [HS^-] + [S^{2-}]$.
[c]The number of *R. pachyptila* worms placed in the aquarium is followed in parentheses by the number that expired during the experiment.

for transcript analysis (see below); those used for isotopic analyses and enzyme assays were freeze-clamped and maintained at −80°C until analysis.

Uptake rates for H_2 and O_2 were calculated using the formula below, where total biomass represents the total weight of the worms without their tubes in each aquarium. Intake and outtake are micromolar concentrations, total mass is in grams, and flow rate is in liters per hour.

$$\left(\frac{\text{intake} - \text{outtake}}{\text{total biomass}}\right) \times \text{flow rate}$$

Dissolved inorganic carbon incorporation by intact *R. pachyptila*. To measure the incorporation of dissolved inorganic carbon (DIC, which is the sum of the species $[CO_2]$, $[HCO_3]$, and $[CO_3^{2-}]$) by intact *R. pachyptila* in the presence of H_2 or sulfide, a 99% $NaH^{13}CO_3$ stock solution was added to the intake tank to achieve a final isotopic composition of 2.64% ^{13}C (of DIC) in the aquarium water. Fluid samples were taken via gastight syringe at the inlet and outlet of the high-pressure aquaria containing the worms, as well as the control vessels that were run without worms. These subsamples were gently filtered through a 0.2-μm cellulose acetate sterile syringe filter, and the filtrate was gently injected into a preevacuated gastight sampling vial (12-ml Exetainer; Labco Inc.). All samples were stored at 4°C and, upon return to the laboratory, were analyzed at the Yale Analytic and Stable Isotope Center (YASIC) on a Deltaplus XP stable isotope ratio mass spectrometer. Posttreatment, worms were quickly dissected and samples of trophosome, plume, and skin were weighed on a microbalance and then frozen at −80°C for later analyses. In the lab, these tissues were lyophilized with a freeze dryer (FreeZone 2.5; Labconco Inc.), acidified with 1 M HCl for ~1 min, rinsed with distilled, deionized water, and dried in a vacuum oven (Labconco Inc.) at 50°C until weights were stable over time, indicating complete drying. Dried samples were then pulverized with a glass mortar and pestle and sent to Boston University Stable Isotope Laboratory, where the samples were weighed into tin boats with a microelectronic balance, combusted in a CN analyzer (Eurovector Inc.), separated chromatographically, and run through a GV Instruments IsoPrime isotope ratio mass spectrometer. $^{13}C/^{12}C$ isotope ratios were measured using the international standards of NBS 20 (Solenhofen Limestone), NBS 21 (spectrographic graphite), and NBS 22 (hydrocarbon oil). $\delta^{13}C_{V\text{-}PDB}$ (per mille) was calculated using the equation below, where R is the atomic ratio ($^{13}C/^{12}C$).

$$\delta^{13}C = \left(\frac{R_{\text{sample}}}{R_{\text{standard}}} - 1\right) \times 1{,}000$$

The rates of DIC incorporation into tissues were calculated from ^{13}C incorporation using a modification of the method in reference 51. The atomic percentages (A%) of labeled and natural abundance samples were calculated from $\delta^{13}C$ values as

$$A\% = \left(\frac{R_{\text{sample}}}{R_{\text{sample}} + 1}\right) \times 100$$

The percentage of ^{13}C that was incorporated into biomass ($^{13}C_{inc}$) was calculated as

$$^{13}C_{\text{inc}} = \left(\frac{A\%_{\text{lab}} - A\%_{\text{nat}}}{A\%_{\text{wat}} - A\%_{\text{nat}}}\right)$$

modified from reference 51, where $A\%_{lab}$ is the atomic percentage of tissue that was incubated in the presence of ^{13}C, $A\%_{nat}$ is the atomic percentage of tissue that was not exposed to the isotopic label, and $A\%_{wat}$ is the atomic percentage of DI^{13}C available in the fluid to which it was exposed. The percent $^{13}C_{inc}$ was multiplied by the dry weight and the percent total carbon of the sample to calculate the weight of the ^{13}C incorporated ($W^{13}C_{inc}$). From this weight of ^{13}C incorporated, a carbon incorporation rate was calculated as described in reference 51.

Dissolved inorganic carbon incorporation by trophosome samples. To determine whether H_2 is used by the symbionts as an electron donor for energy generation, homogenized trophosome was incubated in the presence of this gas and carbon fixation was measured radiometrically. To prepare for this assay, intact *R. pachyptila* worms were incubated in high-pressure respirometers in the presence of H_2 for 2 days (see above). Immediately after *R. pachyptila* worms were removed from the high-pressure aquaria, trophosome was excised, homogenized, and drawn into three glass syringes primed with buffered *R. pachyptila* saline and [^{14}C]bicarbonate as described in reference 52. Dissolved gas concentrations in the syringes consisted of 0.18 mM O_2 and 10 mM DIC; one syringe also had 0.1 mM ΣH_2S, and one had 0.1 mM H_2. Incubations were maintained at 15°C and stirred with magnetic stir bars. Carbon fixation was assayed over 25 min at 5-min intervals. One-hundred-microliter samples were added to 100 μl of 1.2 N HCl to stop the reaction and sparged with air for 2 h to remove remaining $^{14}CO_2$. To minimize quenching, samples were dried and then resuspended in 200 μl of ScintiGest tissue solubilizer (Fisher Chemical) and 20 μl of H_2O_2. After 20 min, 3 ml of ScintiVerse BD cocktail (Fisher Chemical) was added. The following day, radioactivity was measured using a scintillation counter.

A linear regression with indicator variables was used to test whether an electron donor (H_2, ΣH_2S, or none) affected the amount of carbon fixed by the symbionts (IBM SPSS Statistics 24). An F value was calculated from the residual sum of squares from a reduced model ($y = \beta_0 + \beta_1 x_1$, where y = carbon fixed and x_1 = time) and a full model ($y = \beta_0 + \beta_1 x_1 + \beta_2 x_2 + \beta_3 x_3 + \beta_4 x_1 \cdot x_2 + \beta_5 x_1 \cdot x_3$), where x_2 and x_3 are indicator variables for incubations with H_2 and ΣH_2S, respectively.

Hydrogenase assay. A spectrophotometric assay was used to measure hydrogenase activity in the H_2-oxidizing direction via methylene blue reduction (53, 54). For a positive control, *Hydrogenovibrio thermophilus* MA2-6 was batch cultivated under 5% H_2, 5% CO_2, and balance air, harvested via centrifugation (5,000 × *g*, 4°C, and 10 min), and stored at −80°C. Assay buffer (0.1 mM methylene blue, 20 mM

KH_2PO_4 [pH 7] with KOH) was sparged overnight with argon in a glove bag. On the day of the assay, crude cell extracts were prepared from *H. thermophilus* and *R. pachyptila* trophosome samples by thawing them in the glove bag and disrupting them with a mortar and pestle in assay buffer. Samples (0.1 ml) and 0.9 ml of assay buffer were sealed in glass cuvettes with septa. After injecting the appropriate headspace (H_2, or argon for negative controls), cuvettes were agitated and removed from the glove bag, and methylene blue reduction was monitored at 601 nm ($\varepsilon = 7{,}000\ mol^{-1}cm^{-1}$). Protein concentrations in the assays were measured with an RC DC protein assay (Bio-Rad, Inc.). For the positive control, to determine whether the presence of H_2 affected the rate of methylene blue reduction, a linear regression with indicator variables was used as described above for dissolved inorganic carbon incorporation by trophosome samples.

Bioinformatics. Genes encoding hydrogenase and hydrogenase-associated proteins were collected from "*Ca*. Endoriftia persephone" genome data (*R. pachyptila* host [27, 28] or *Ridgeia piscesae* and *Tevnia jerichonana* hosts [55]; available through NCBI and the JGI Integrated Microbial Genomes & Microbiomes system). Hydrogenase sequences were classified using HydDB (https://services.birc.au.dk/hyddb/) (56).

Abundances of hydrogenase transcripts. Trophosome tissue was quickly excised from three responsive tubeworms from each treatment for mRNA transcript abundance analyses. These tissues were homogenized with a stainless steel rotor-stator Tissue-Tearor (Cole Palmer) in 1 ml of TRIzol reagent and maintained at −80°C. Total RNA was extracted using Direct-zol RNA MiniPrep (Zymo Research), following the manufacturer's instructions. Normalized total RNA was sent to the Microbial 'Omics Core (MOC) at the Broad Institute for library preparation and sequencing. After barcoded adaptor ligation and rRNA depletion, cDNA libraries were constructed from 0.5 to 1 μg of total RNA, using a modified RNAtag-seq protocol (57). In short, after reverse transcription, an adaptor was added to the 3′ end of the cDNA by template switching using SMARTScribe (Clontech) (58). cDNA was sequenced with a 2×33- to 75-bp paired-end protocol with the Illumina Novaseq 6000 platform. After sequencing, transcripts were quality assessed using FastQC (https://www.bioinformatics.babraham.ac.uk/projects/fastqc/), overrepresented reads were removed (https://github.com/harvardinformatics/TranscriptomeAssemblyTools), and reads were quality trimmed using TrimGalore (https://github.com/FelixKrueger/TrimGalore). The abundance of transcripts from each sample was pseudoaligned against the published coding regions (CDS) of the genome for "*Ca*. Endoriftia persephone" (28) with kallisto (59).

Four comparisons of transcript abundances in trophosome samples were undertaken in R using sleuth (60): (i) *R. pachyptila* incubated under high-O_2 conditions with H_2 versus ΣH_2S, (ii) *R. pachyptila* incubated under low-O_2 conditions with H_2 versus ΣH_2S, (iii) *R. pachyptila* incubated with H_2 under high-O_2 versus low-O_2 conditions, and (iv) *R. pachyptila* incubated with ΣH_2S under high-O_2 versus low-O_2 conditions. These comparisons were done with the Wald test to calculate β values, using log-transformed data so that the β values represent an estimate of $\log_2$ fold change between treatments. Values of *P* were adjusted for false discovery using the Benjamini-Hochberg method (61), with a significance cutoff value for *P* adjusted (qval) of ≤ 0.05.

SUPPLEMENTAL MATERIAL

Supplemental material is available online only.

SUPPLEMENTAL FILE 1, PDF file, 0.1 MB.

ACKNOWLEDGMENTS

We are very grateful to the captain, pilots, and crew of the *R/V Atlantis* and HOV *Alvin*. We are also grateful to Roxanne Beinart, Kiana Frank, Amy Gartman, and Jon Sanders for their assistance with these experiments.

We are also grateful for support from the National Science Foundation (NSF-IOS-1257532 to K.M.S. and NSF-IOS-1257755 to P.R.G.) and to the anonymous reviewers for their helpful comments.

J.H.M., J.M.L., K.M.S., and P.R.G. designed this study; J.H.M., J.M.L., J.D., and K.M.S. conducted experiments and contributed to data analysis; and J.H.M., J.M.L., K.M.S., and P.R.G. wrote the report.

REFERENCES

1. Petersen JM, Zielinski FU, Pape T, Seifert R, Moraru C, Amann R, Hourdez S, Girguis PR, Wankel SD, Barbe V, Pelletier E, Fink D, Borowski C, Bach W, Dubilier N. 2011. Hydrogen is an energy source for hydrothermal vent symbioses. Nature 476:176–180. https://doi.org/10.1038/nature10325.
2. Kleiner M, Wentrup C, Lott C, Teeling H, Wetzel S, Young J, Chang Y-J, Shah M, VerBerkmoes NC, Zarzycki J, Fuchs G, Markert S, Hempel K, Voigt B, Becher D, Liebeke M, Lalk M, Albrecht D, Hecker M, Schweder T, Dubilier N. 2012. Metaproteomics of a gutless marine worm and its symbiotic microbial community reveal unusual pathways for carbon and energy use. Proc Natl Acad Sci U S A 109:E1173–E1182. https://doi.org/10.1073/pnas.1121198109.
3. Goffredi SK, Wilpiszeski R, Lee R, Orphan VJ. 2008. Temporal evolution of methane cycling and phylogenetic diversity of archaea in sediments from a deep-sea whale-fall in Monterey Canyon, California. ISME J 2:204. https://doi.org/10.1038/ismej.2007.103.
4. Amend JP, McCollom TM, Hentscher M, Bach W. 2011. Catabolic and anabolic energy for chemolithoautotrophs in deep-sea hydrothermal systems hosted in different rock types. Geochim Cosmochim Acta 75:5736–5748. https://doi.org/10.1016/j.gca.2011.07.041.
5. Hentscher M, Bach W. 2012. Geochemically induced shifts in catabolic energy yields explain past ecological changes of diffuse vents in the East Pacific Rise 9°50′N area. Geochem Trans 13:2. https://doi.org/10.1186/1467-4866-13-2.
6. Wankel SD, Germanovich LN, Lilley MD, Genc G, DiPerna CJ, Bradley AS,

Olson EJ, Girguis PR. 2011. Influence of subsurface biosphere on geochemical fluxes from diffuse hydrothermal fluids. Nat Geosci 4:461. https://doi.org/10.1038/ngeo1183.
7. McNichol J, Sylva SP, Thomas F, Taylor CD, Sievert SM, Seewald JS. 2016. Assessing microbial processes in deep-sea hydrothermal systems by incubation at in situ temperature and pressure. Deep Sea Res Part 1 Oceanogr Res Pap 115:221–232. https://doi.org/10.1016/j.dsr.2016.06.011.
8. Pjevac P, Meier DV, Markert S, Hentschker C, Schweder T, Becher D, Gruber-Vodicka HR, Richter M, Bach W, Amann R, Meyerdierks A. 2018. Metaproteogenomic profiling of microbial communities colonizing actively venting hydrothermal chimneys. Front Microbiol 9:680. https://doi.org/10.3389/fmicb.2018.00680.
9. Ver Eecke HC, Butterfield DA, Huber JA, Lilley MD, Olson EJ, Roe KK, Evans LJ, Merkel AY, Cantin HV, Holden JF. 2012. Hydrogen-limited growth of hyperthermophilic methanogens at deep-sea hydrothermal vents. Proc Natl Acad Sci U S A 109:13674–13679. https://doi.org/10.1073/pnas.1206632109.
10. Vignais PM, Billoud B. 2007. Occurrence, classification, and biological function of hydrogenases: an overview. Chem Rev 107:4206–4272. https://doi.org/10.1021/cr050196r.
11. Vignais P, Billoud B, Meyer J. 2001. Classification and phylogeny of hydrogenases. FEMS Microbiol Rev 25:455–501. https://doi.org/10.1111/j.1574-6976.2001.tb00587.x.
12. Rowe AR, Xu S, Gardel E, Bose A, Girguis P, Amend JP, El-Naggar MY. 2019. Methane-linked mechanisms of electron uptake from cathodes by *Methanosarcina barkeri*. mBio 10:e02448-18. https://doi.org/10.1128/mBio.02448-18.
13. Cracknell JA, Vincent KA, Armstrong FA. 2008. Enzymes as working or inspirational electrocatalysts for fuel cells and electrolysis. Chem Rev 108:2439–2461. https://doi.org/10.1021/cr0680639.
14. Buckel W, Thauer RK. 2018. Flavin-based electron bifurcation, ferredoxin, flavodoxin, and anaerobic respiration with protons (Ech) or NAD(+) (Rnf) as electron acceptors: a historical review. Front Microbiol 9:401. https://doi.org/10.3389/fmicb.2018.00401.
15. Goldet G, Wait AF, Cracknell JA, Vincent KA, Ludwig M, Lenz O, Friedrich B, Armstrong FA. 2008. Hydrogen production under aerobic conditions by membrane-bound hydrogenases from *Ralstonia* species. J Am Chem Soc 130:11106–11113. https://doi.org/10.1021/ja8027668.
16. Hexter SV, Grey F, Happe T, Climent V, Armstrong FA. 2012. Electrocatalytic mechanism of reversible hydrogen cycling by enzymes and distinctions between the major classes of hydrogenases. Proc Natl Acad Sci U S A 109:11516–11521. https://doi.org/10.1073/pnas.1204770109.
17. Orengo CA, Thornton JM. 2005. Protein families and their evolution-a structural perspective. Annu Rev Biochem 74:867–900. https://doi.org/10.1146/annurev.biochem.74.082803.133029.
18. Dubilier N, Bergin C, Lott C. 2008. Symbiotic diversity in marine animals: the art of harnessing chemosynthesis. Nat Rev Microbiol 6:725–740. https://doi.org/10.1038/nrmicro1992.
19. Bright M, Keckeis H, Fisher CR. 2000. An autoradiographic examination of carbon fixation, transfer and utilization in the *Riftia pachyptila* symbiosis. Mar Biol 136:621–632. https://doi.org/10.1007/s002270050722.
20. Fisher CR, Childress JJ. 1986. Translocation of fixed carbon from symbiotic bacteria to host tissues in the gutless bivalve, *Solemya reidi*. Mar Biol 93:59–68. https://doi.org/10.1007/BF00428655.
21. Fisher CR, Childress JJ. 1992. Organic carbon transfer from methanotropic symbionts to the host hydrocarbon-seep mussel. Symbiosis 12:221–235.
22. Volland JM, Schintlmeister A, Zambalos H, Reipert S, Mozetic P, Espada-Hinojosa S, Turk V, Wagner M, Bright M. 2018. NanoSIMS and tissue autoradiography reveal symbiont carbon fixation and organic carbon transfer to giant ciliate host. ISME J 12:714–727. https://doi.org/10.1038/s41396-018-0069-1.
23. Girguis PR, Childress JJ. 2006. Metabolite uptake, stoichiometry and chemoautotrophic function of the hydrothermal vent tubeworm *Riftia pachyptila*: responses to environmental variations in substrate concentrations and temperature. J Exp Biol 209:3516–3528. https://doi.org/10.1242/jeb.02404.
24. Stewart FJ, Newton IL, Cavanaugh CM. 2005. Chemosynthetic endosymbioses: adaptations to oxic-anoxic interfaces. Trends Microbiol 13:439–448. https://doi.org/10.1016/j.tim.2005.07.007.
25. Kleiner M, Wentrup C, Holler T, Lavik G, Harder J, Lott C, Littmann S, Kuypers MMM, Dubilier N. 2015. Use of carbon monoxide and hydrogen by a bacteria-animal symbiosis from seagrass sediments. Environ Microbiol 17:5023–5035. https://doi.org/10.1111/1462-2920.12912.
26. Markert S, Arndt C, Felbeck H, Becher D, Sievert SM, Hügler M, Albrecht D, Robidart J, Bench S, Feldman RA, Hecker M, Schweder T. 2007. Physiological proteomics of the uncultured endosymbiont of *Riftia pachyptila*. Science 315:247–250. https://doi.org/10.1126/science.1132913.
27. Robidart JC, Bench SR, Feldman RA, Novoradovsky A, Podell SB, Gaasterland T, Allen EE, Felbeck H. 2008. Metabolic versatility of the Riftia pachyptila endosymbiont revealed through metagenomics. Environ Microbiol 10:727. https://doi.org/10.1111/j.1462-2920.2007.01496.x.
28. Gardebrecht A, Markert S, Sievert SM, Felbeck H, Thurmer A, Albrecht D, Wollherr A, Kabisch J, Le Bris N, Lehmann R, Daniel R, Liesegang H, Hecker M, Schweder T. 2012. Physiological homogeneity among the endosymbionts of Riftia pachyptila and Tevnia jerichonana revealed by proteogenomics. ISME J 6:766–776. https://doi.org/10.1038/ismej.2011.137.
29. Cavanaugh CM, Gardiner SL, Jones ML, Jannasch HW, Waterbury JB. 1981. Prokaryotic cells in the hydrothermal vent tube worm *Riftia pachyptila* Jones: possible chemoautotrophic symbionts. Science 213:340–342. https://doi.org/10.1126/science.213.4505.340.
30. Felbeck H, Childress JJ, Somero GN. 1981. Calvin-Benson cycle and sulfide oxidation enzymes in animals from sulfide-rich habitats. Nature 293:291–293. https://doi.org/10.1038/293291a0.
31. Distel DL, Lane DJ, Olsen GJ, Giovannoni SJ, Pace B, Pace NR, Stahl DA, Felbeck H. 1988. Sulfur-oxidizing bacterial endosymbionts: analysis of phylogeny and specificity by 16S rRNA sequences. J Bacteriol 170:2506–2510. https://doi.org/10.1128/jb.170.6.2506-2510.1988.
32. Fisher CR, Childress JJ, Minnich E. 1989. Autotrophic carbon fixation by the chemoautotrophic symbionts of *Riftia pachyptila*. Biol Bull 177:372–385. https://doi.org/10.2307/1541597.
33. Arp AJ, Childress JJ. 1981. Blood function in the hydrothermal vent vestimentiferan tube worm. Science 213:342–344. https://doi.org/10.1126/science.213.4505.342.
34. Childress JJ, Arp AJ, Fisher CR. 1984. Metabolic and blood characteristics in the hydrothermal vent tube-worm *Riftia pachyptila*. Mar Biol 83:109–124. https://doi.org/10.1007/BF00394718.
35. Fisher CR, Childress JJ, Arp AJ, Brooks JM, Distel D, Favuzzi JA, Macko SA, Newton A, Powell MA, Somero GN, Soto T. 1988. Physiology, morphology, and biochemical composition of *Riftia pachyptila* at Rose Garden in 1985. Deep Sea Res 35:1745–1758. https://doi.org/10.1016/0198-0149(88)90047-7.
36. Vetter RD, Fry B. 1998. Sulfur contents and sulfur-isotope compositions of thiotrophic symbioses in bivalve molluscs and vestimentiferan worms. Mar Biol 132:453–460. https://doi.org/10.1007/s002270050411.
37. Fisher CR, Childress JJ. 1984. Substrate oxidation by trophosome tissue from *Riftia pachyptila* Jones (phylum Pogonophora). Mar Biol Lett 5:171–183.
38. Childress JJ, Fisher CR, Favuzzi JA, Kochevar RE, Sanders NK, Alayse AM. 1991. Sulfide-driven autotrophic balance in the bacterial symbiont-containing hydrothermal vent tubeworm, *Riftia pachyptila* Jones. Biol Bull 180:135–153. https://doi.org/10.2307/1542437.
39. VonDamm KL, Lilley MD. 2004. Diffuse flow hydrothermal fluids from 9°50′N East Pacific Rise: origin, evolution and biogeochemical controls, p 245–268. *In* Wilcock WSD, DeLong EF, Kelley DS, Baross JA (ed), Subseafloor biosphere at mid-ocean ridges. American Geophysical Union, Washington, DC.
40. Holm S. 1979. A simple sequentially rejective multiple test procedure. Scand J Stat 6:65–70.
41. Li Y, Liles MR, Halanych KM. 2018. Endosymbiont genomes yield clues of tubeworm success. ISME J 12:2785–2795. https://doi.org/10.1038/s41396-018-0220-z.
42. Fox JD, Kerby RL, Roberts GP, Ludden PW. 1996. Characterization of the CO-induced, CO-tolerant hydrogenase from Rhodospirillum rubrum and the gene encoding the large subunit of the enzyme. J Bacteriol 178:1515–1524. https://doi.org/10.1128/jb.178.6.1515-1524.1996.
43. Maness PC, Weaver PF. 2001. Evidence for three distinct hydrogenase activities in *Rhodospirillum rubrum*. Appl Microbiol Biotechnol 57:751–756. https://doi.org/10.1007/s00253-001-0828-0.
44. Feldman R, Black M, Cary C, Lutz R, Vrijenhoek R. 1997. Molecular phylogenetics of bacterial endosymbionts and their vestimentiferan hosts. Mol Mar Biol Biotechnol 6:268–277.
45. Harmer TL, Rotjan RD, Nussbaumer AD, Bright M, Ng AW, DeChaine EG. 2008. Free-living tube worm endosymbionts found at deep-sea vents.

Appl Environ Microbiol 74:3895–3898. https://doi.org/10.1128/AEM.02470-07.
46. Greening C, Biswas A, Carere CR, Jackson CJ, Taylor MC, Stott MB, Cook GM, Morales SE. 2016. Genomic and metagenomic surveys of hydrogenase distribution indicate H2 is a widely utilised energy source for microbial growth and survival. ISME J 10:761–777. https://doi.org/10.1038/ismej.2015.153.
47. Ma K, Schicho RN, Kelly RM, Adams MW. 1993. Hydrogenase of the hyperthermophile *Pyrococcus furiosus* is an elemental sulfur reductase or sulfhydrogenase: evidence for a sulfur-reducing hydrogenase ancestor. Proc Natl Acad Sci U S A 90:5341–5344. https://doi.org/10.1073/pnas.90.11.5341.
48. Berney M, Greening C, Conrad R, Jacobs WR, Jr, Cook GM. 2014. An obligately aerobic soil bacterium activates fermentative hydrogen production to survive reductive stress during hypoxia. Proc Natl Acad Sci U S A 111:11479–11484. https://doi.org/10.1073/pnas.1407034111.
49. Cline JD, Richards FA. 1969. Oxygenation of hydrogen sulfide in seawater at constant salinity, temperature and pH. Environ Sci Technol 3:838–843. https://doi.org/10.1021/es60032a004.
50. Childress JJ, Mickel TJ. 1980. A motion compensated shipboard precision balance system. Deep Sea Res 27A:965–970. https://doi.org/10.1016/0198-0149(80)90008-4.
51. Beinart RA, Gartman A, Sanders JG, Luther GW, Girguis PR. 2015. The uptake and excretion of partially oxidized sulfur expands the repertoire of energy resources metabolized by hydrothermal vent symbioses. Proc Biol Sci 282:20142811. https://doi.org/10.1098/rspb.2014.2811.
52. Scott KM, Boller AJ, Dobrinski KP, Le Bris N. 2012. Response of hydrothermal vent vestimentiferan *Riftia pachyptila* to differences in habitat chemistry. Mar Biol 159:435–442. https://doi.org/10.1007/s00227-011-1821-5.
53. Adams MWW, Hall DO. 1979. Purification of the membrane-bound hydrogenase of *Escherichia coli*. Biochem J 183:11–22. https://doi.org/10.1042/bj1830011.
54. Ren Q, Paulsen IT. 2005. Comparative analysis of fundamental differences in membrane transport capabilities in prokaryotes and eukaryotes. PLoS Comp Biol 1:e27. https://doi.org/10.1371/journal.pcbi.0010027.
55. Perez M, Juniper KS. 2016. Insights into symbiont population structure among three vestimentiferan tubeworm host species at Eastern Pacific spreading centers. Appl Environ Microbiol 82:5197–5205. https://doi.org/10.1128/AEM.00953-16.
56. Søndergaard D, Pedersen CNS, Greening C. 2016. HydDB: a web tool for hydrogenase classification and analysis. Sci Rep 6:34212. https://doi.org/10.1038/srep34212.
57. Shishkin AA, Giannoukos G, Kucukural A, Ciulla D, Busby M, Surka C, Chen J, Bhattacharyya RP, Rudy RF, Patel MM, Novod N, Hung DT, Gnirke A, Garber M, Guttman M, Livny J. 2015. Simultaneous generation of many RNA-seq libraries in a single reaction. Nat Methods 12:323–325. https://doi.org/10.1038/nmeth.3313.
58. Zhu YY, Machleder EM, Chenchik A, Li R, Siebert PD. 2001. Reverse transcriptase template switching: a SMART approach for full-length cDNA library construction. Biotechniques 30:892–897. https://doi.org/10.2144/01304pf02.
59. Bray NL, Pimentel H, Melsted P, Pachter L. 2016. Near-optimal probabilistic RNA-seq quantification. Nat Biotechnol 34:525–527. https://doi.org/10.1038/nbt.3519.
60. Pimentel HJ, Bray N, Puente S, Melsted P, Pachter L. 2017. Differential analysis of RNA-Seq incorporating quantification uncertainty. Nat Methods 14:687–690. https://doi.org/10.1038/nmeth.4324.
61. Benjamini Y, Hochberg Y. 1995. Controlling the false discovery rate: a practical and powerful approach to multiple testing. J R Stat Soc B 57:289–300. https://doi.org/10.1111/j.2517-6161.1995.tb02031.x.